Chapter I

Growth of Cr-doped CdTe quantum dots

The aim of this thesis was to study the dynamic of single spin in quantum dots. The first step in this study was to grow these system. We studied to type of quantum dots: self assembled QDs and strain free QDs. The strained dots are formed by the partial relaxation of a CdTe layer on ZnTe. Strain free dots are formed by thickness variation of a CdTe quantum well between CdMgTe barriers. The growth of Cr doped samples were done in Pr. Shinji Kuroda laboratory, in the University of Tsukuba. The Mn-doped samples were grown at Grenoble, in the INAC, by Dr. Hervé Boukari.

We will focus in this chapter on the growth done at Tsukuba by Molecular Beam Epitaxy (MBE). We begin by giving some general explanation on the MBE process and the different tools that are used in it. We then go to the growth of the self-assembled quantum dots, detailing the preparation of the substrate and the actual growth, and discussing quickly the results. In the last section, we present two other kind of sample we grew: samples with the possibility of applying an electric field on them, and the strain free dots. For each of them, we detail the growth process and discuss the results we had studying them.

I.1   Generality on Molecular Beam Expitaxy

In the MBE process, cells of pure elements are heated to control their evaporation or until they reach sublimation. Those elements will formed the desired crystal on the substrate. They are kept in Knudsen cell, which consist of a crucibles of high-melting-point material with a low contaminating power (typically Pyrolytic Boron Nitride) wrapped in tungsten filament which will act as heater. Each are closed by a shutter controlled by a computer.

Upon reaching the right temperature, said shutter is opened to let the element travel to the substrate. The the camber containing the substrate is kept in Ultra High Vacuum (about 10^{-8} Pa), in order to avoid contamination of the sample and get a mean free path of the gas long compared to distance to the sample. This process is illustrated on Fig. I.1. Reaching the surface, the atoms diffuse before stopping, either having dissipated their kinetic through interaction with the surface, or (more commonly) being kept by island of previously deposited atoms. In the ideal case, the growth occur layer by layer, slowly (about 1 monolayer/s), giving a good control of the thickness of the grown material.
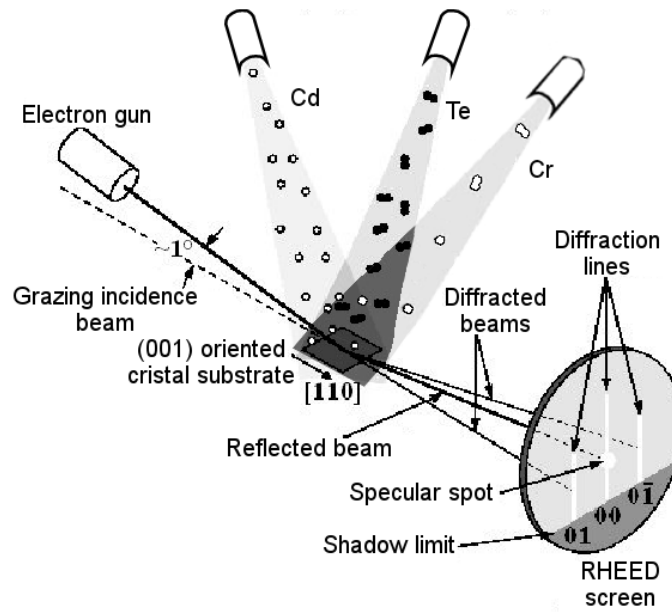

Figure I.1: Scheme of a MBE chamber and the position of the cells in regard of the substrate.

This necessity of Ultra High Vacuum kept the MBE to be developed before the end of the 1960s [1], although the the idea was formalized at the end of the 19th century. This method offers a good control on the growth, which make it useful for the development of nanostructure and nanoscience. The deposition layer by layer give the possibility to grow really thin structure, and the transition between two materials can be really abrupt, on a few monolayer (ML). Growing nano-structure is still the main use of MBE. However, this method is mainly on research purpose, its slow growth speed and hard to fulfil growth conditions being an obstacle for the industrialization of the process.

CdTe growth in MBE is *auto-regulated*: if only one element is open, only a

given quantity of material will be deposited and then the growth will stop until the other element is also deposited. The deposited quantity of material before the growth stop depends only on the substrate temperature. This allows us to achieve a really fine control of the growth using the MBE mode called Atomic Layer Epitaxy (ALE) or Migration-Enhanced Epitaxy (MEE). In this mode, only one element is opened at a time, growing the sample really layer by layer. Between each opening, the sample is left under vacuum in order to relax the surface. A full cycle correspond to opening each cell once. For CdTe, a substrate temperature between 260°C and 290°C guaranty a growth of only 0.5 ML for each cycle [2]. This allow a small uncertainty on the substrate temperature while keeping a really good control on the growth of the sample.

The growth was monitored with RHEED (Reflexion High-Energy Electron Diffraction). This technique requires a high vacuum, a given since MBE ask for ultra-high vacuum condition, and the use of an electron gun able to produce high energy electron. The beam of the gun is sent at low angle, between 1° and 3°, to the surface sample. This way, the electrons will only probe the surface of the sample, entering the material only on a 3 or 4 ML. Therefore the detected pattern directly gives information on the flatness and the crystallinity of the surface.

Incident electrons have a wave vector $\mathbf{k_i} = 2\pi/\lambda_e$, with λ_e the electron wavelength, typically 6 or 7 pm for an electron gun energy between 30 and 40 kV. Since only scattered diffraction is considered, the diffracted wave vector $\mathbf{k_f}$ as the same norm as the incident one $\mathbf{k_i}$. So the Ewald's Sphere has a radius equal to the norm of $\mathbf{k_i}$. In the reciprocal space, the plane of diffraction are infinite line. So, in the case of a perfect crystal, with a a perfect detector, the intersection with Ewald's sphere should be points. However, since the crystal can have some defect and neither the gun or the detector are perfect, the diffracted pattern present line, such as visible on Fig.I.3(b).

Once dots are grown, though, the surface become rough at the scale of the length of coherence of the beam. The electrons can interact with several more layer while passing through the dots. This can be seen on the diffraction pattern, where lines become points, such as shown on Fig.I.3(e).

Another use of the RHEED diffraction is the monitoring of the number of layer grown through ALE. Focusing on the lowest angle reflected spot, called the specular spot, one can see small variation in the reflected intensity during the growth, such as presented on Fig.I.2. This intensity is minimal when there is half a ML grown, and maximal when the ML is fully grown. This is due to the variation of reflectivity of the surface: maximal for a flat surface, minimal for a rough one. Therefore, a period of these oscillation is exactly the growth of a single monolayer [3, 4]. We can also see the relaxation of a layer, if the variation of
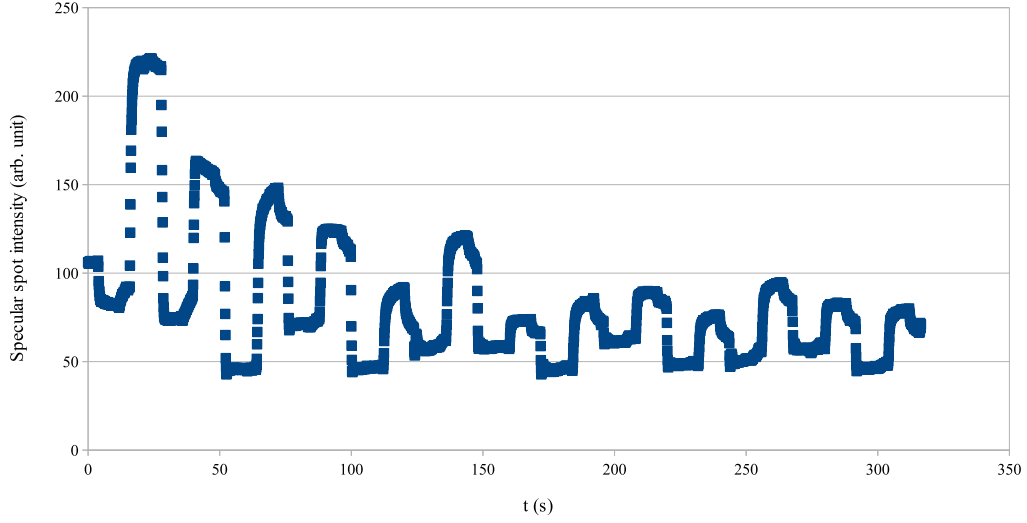
intensity disappear at a point.

Figure I.2: RHEED oscillation for the ALE of strained dots.

I.2 Strained dots: CdTe/ZnTE

I.2.1 Substrate preparation

The sample was grown on ZnTe(100) substrates. In order to get the bes surface to grow on, we need to clean the sample. Two cleaning methods were tested: etching of the sample in a Bromure solution, and exposition of the sample to a hydrogen radical plasma.

The etching process was done in four steps. All of them, except the etching in Bromure-ethanol, occur in an ultrasonic cleaning device vibrating the sample at 43kHz and last 3 minutes. We began with a cleaning in acetone, followed by one in ethanol. The third step was the actual etching: the substrate was put in a solution of Bromure-ethanol, with 3% of Bromure, during 1 minute. We finally rinsed it in methanol. Once rinsed, we keep the sample in ethanol until fixing them to the sample holder. The growth usually occur the day after the cleaning, the sample being kept in the MBE load-lock chamber, under vacuum.

Another type of cleaning of the surface was tried: using hydrogen radical (H*) to remove the impurity at the surface. This was done to get a smoother surface directly in the chamber, to avoid any contamination by the atmosphere that might occur during the transport from the etching room to the MBE chamber. In order to

form the radical gas, a hydrogen gas was ionized in a chamber by a RF power source of 300 W and with a frequency of 13.6 MHz. This gas composition is optically checked by probing the emission of the Balmer series: for a pure hydrogen gas, peaks at 656 nm and 486 nm appear clearly. During the formation of this gas, the substrate temperature is raised to 400°C and we initiate its rotation. Once the plasma is formed, the valve to the main chamber is opened and the substrate is exposed to the plasma for 15 minutes. In order to check the quality of the surface, we look at the RHEED that should present strike.

I.2.2   Strained dots growth

The targeted flux chosen for the growth of the CdTe/ZnTe QD are presented in Tab. I.1 for each cell used during the growth of strained QDs. These flux were measured via the pressure gauge inside the MBE chamber. It was shown that the best quality of ZnTe was achieved for a growth in excess of Zn [5]. Otherwise, vacancies appear in the bulk, optically visible, and the surface is more rough. Moreover, the adsorption power of the Zn is smaller than the Te. For these reason, we choose to grow the ZnTe barriers in excess of Zn.

Table I.1: Aimed flux for each cell during the growth of the strained QDs.

Elements	Targeted BEP (Torr)
Cd	4.5×10^{-7}
Te	4.5×10^{-7}
Zn	6.8×10^{-7}

As previously stated, the CdTe quantum dots was grown using ALE. In this mode, the flux of the elements does not affect the quantity of element deposited at each cycle, as long as their flux is high enough to complete the maximal thickness for the chosen substrate temperature. Therefore, the flux for both of the compounds are therefore chosen to be the same [2].

Beginning the growth, the substrate temperature was initially raised to 415°C. The Zn cell shutter was open starting at 360°C, in order to flatten the surface for the growth. While it took several minutes to raise the substrate temperature, only one Zn layer was deposited due to the auto-regulation of the growth. When the substrate temperature reach 415°C, the Te shutter was also open, in order to grow the ZnTe buffer layer. This thick ZnTe layer guaranteed us to the best possible surface for the growth of the QD layer [6]. Once done, we set up the RHEED, growing a few more ZnTe level while searching the specular spot. The substrate temperature was then lowered to 295°C, the Zn cell being open until the temperature reach 360°C.
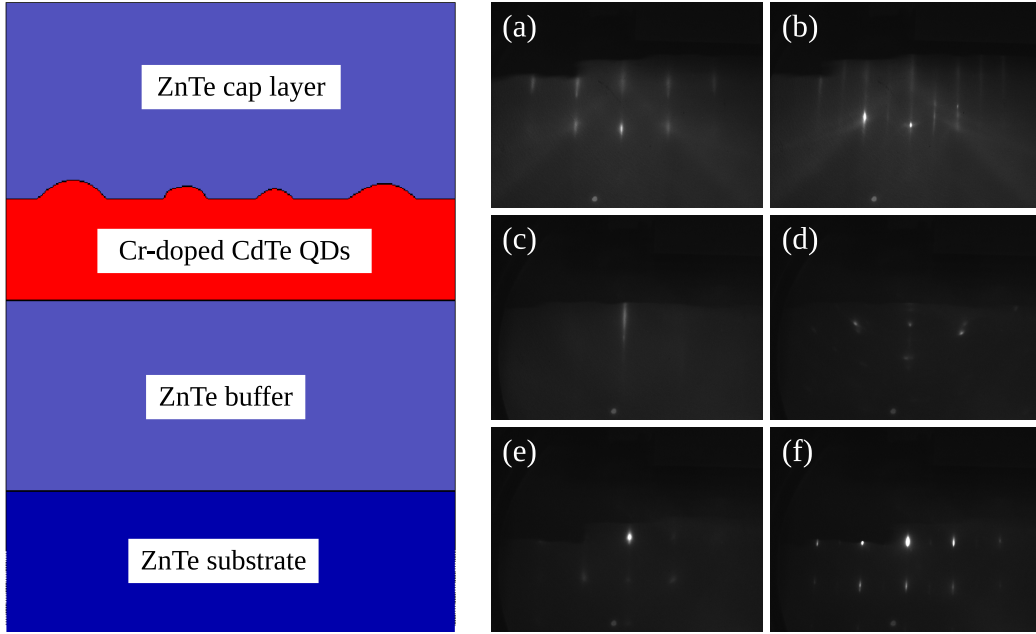
Figure I.3: Left: Layer structure of the strain Cr-doped CdTe QDs samples. Right: RHEED pattern taken at different key moment of the growth: (a) before the growth of the ZnTe buffer, (b) after the growth of the ZnTe buffer, (c) after the (Cd,Cr)Te ALE, (d) after the Te deposition, (e) during the Te evaporation (the picture was taken at $T_{substrate} = 177°C$) and (f) after the growth of the ZnTe cap.

One of the main difficulty of this work was to calibrate the Cr flux in order to embed only a single Cr atom in most of the QDs of the sample. To achieve this, the Cr density must be of the same order as the QDs density at the surface of the sample. This means a really small flux, with a BEP of the magnitude of 10^{-10} Torr, which is about one order lower than the main chamber pressure and therefore not measurable with our technique. The optimisation was done starting with the know how acquired in Grenoble on the Mn and trying to optimise it for the Tsukuba machine, through a feedback loop with the micro-PL characterization in Grenoble.

This really small flux was achieved by heating the Cr cell around 1000K, low compared to its sublimation temperature, and opening the cell only once during the ALE, for only 5s. In order to have big enough QDs, emitting at right wavelengths, 6.5 ML of CdTe is the optimal CdTe thesis. However, the critical thickness of CdTe on ZnTe is 6.5 ML. Dislocations and defect will form in the layer for a higher thickness. Therefore, some sample were also grown with a 5.5 ML thickness in order to not get too close to the limit. At the chosen temperature, it correspond

6

to either 13 cycles of ALE (for 6.5 ML) or 11 cycles (for 5.5 ML). The Cr cells was opened during the 7th cycle, halfway through the growth of the QD layer, in order to allow the Cr atoms to diffuse without going out the QD layers. The whole ALE recipe to grow the QDs layer is given in the Fig.I.4.
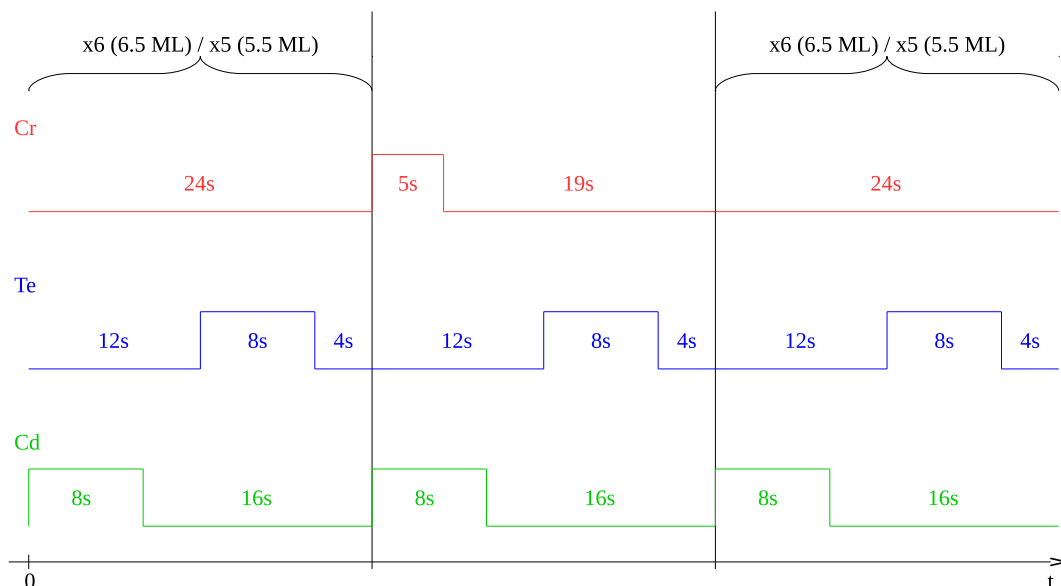

Figure I.4: Opening and closing cycles of each cell for the ALE of strained (Cd,Cr)Te samples.

After the growth of the CdTe layer, we lowered the substrate temperature to 210°C to deposit the Te layer. It was deposited during 5 minutes. This step allows the CdTe layer to relax and form the quantum dots [7]. We then heated up the substrate again until 320°C, were we stayed for 20s in order to evaporate all the deposited Te [8]. If the dots were formed, we saw a spotty pattern like the one presented on Fig. I.3 (f). The Zn and Te cells were then opened, while the substrate temperature was raised to 350°C in order to grow a protective layer above the QDs.

I.2.3 Results

Cr-samples were grown in the University of Tsukuba and studied in Grenoble, at the Neel institute, via micro-photoluminescence (μ-PL). A high refractive index hemi-spherical Solid Immersion Lens (SIL) was mounted on the sample before their study, to improve the spatial resolution and enhance the collection efficiency of a single dot PL in a low temperature (T = 5K) optical microscope.

Table I.2: List of samples where Cr was found.

Sample	Cleaning process	CdTe MLs	Cr aimed concentration (%)
dot358	Br etching	6.5	0.06
dot359	Br etching	6.5	0.11
dot363	Br etching	6.5	0.21
dot383	Br etching	5.5	0.19
dot385	Br etching	5.5	0.17

The characterization of the samples came in two times. First, we took macro-photoluminescence spectra, on a large energy range, typically between 1.8 and 2.3 eV, with a laser exciting at 2.9 eV. This allow us to test the luminescence of the sample: if the Cr concentration is too high, it may kill the PL of the dot layer, and thus it will not be seen in the macro-PL. If this luminescence is seen, the sample is then studied by μ-PL, on a much narrower energy band (about 10 meV), in order to be able to study a dot individually. We scan randomly the sample, searching for dots. We judge the quality of the sample by the proportion of thin emission peaks versus broad one, large quantity of broad peaks hinting at a high Cr concentration, and by the number of actual Cr-doped dots we found.

The samples where the Cr concentration was found to be good are listed in Tab. I.2. The Cr concentration was estimated using the Cr flux and the known Mn concentration in CdTe in function of the flux of Mn during the growth. Since the Cr flux can't be measured, it was estimated using Arrhenius law. We see that, for most of the sample, the aimed Cr concentration is above 0.15%. dot358 and dot359 had a lower aimed Cr concentration, but, even though some good dots were found in them, the probability to find one were still low. Tests were done with an aimed Cr concentration at 0.25%, but no luminescence were found in the dot layer. Therefore, in order to maximize the probability of finding a dot with a single Cr and keeping a good PL, we settled for an aimed Cr concentration of 0.17%.

I.3   Other kind of samples

I.3.1   Charge control samples

Charge control samples are pretty straightforward. Instead of growing the sample on a non-doped ZnTe substrate, we do the growth on p-doped ZnTe substrate. Same steps are followed, but with thinner buffer and cap layers, in order to have a stronger electric on the dot layer. We chose to do both about 150 nm thick,

Gold deposition time (s)	Resistance (Ω)
15	300
20	80
25	25
30	20
35	0
60	0

Figure I.5: Measured conductivity of the Au layer on GaAs for different deposition time.

calibrating with the ZnTe growth speed calculated via the RHEED oscillations.

Once the growth were finished, a thin, semi-transparent gold layer is deposited by sputtering. The samples are kept in nitrogen atmosphere during the transport. The exposition time of the sample in the sputtering machine was calibrated using gold deposited on GaAs substrate. Resistance of the gold layer was measured. Results are presented in Tab. I.5. In order to keep a collection of the light emitted by the quantum, a thin layer was necessary. However, we also needed a gold layer thick enough to cover the entire surface of the sample. These considerations lead us to chose a deposition time of 35 s.

Results

We successfully grew this kind of sample and studied them with μPL. We were able to look at the luminescence of a dot and see the evolution of its PL under the application of an bias voltage. Fig. I.6 (a) presents the results of such an experiment.

The main result of the experiment is the apparition of different species depending on the applied electric field. We see for example that, for a bias voltage of $+3$ V (Fig. I.6 (b)), the neutral species are almost extinguish and the charged species X^+, X^{++} and X_2^+ have the more intense PL. Similarly, at negative electric field, only the charged species X^-, X^{--} and X_2^- remain, X^{--} and X_2^- disappearing for an applied bias voltage higher than -2 V. This shows that we can select efficiently the charge of a studied quantum dot applying a bias voltage on it.

Only one charged sample containing Cr atoms was studied: dot390. It was cleaned by H* plasma. The QD layer was 5.5 ML thick and the Cr concentration was aimed to be 0.16%. However, no Cr doped quantum dots were found. Some dots presenting a emission close to the one expected for Cr atoms were found, but they were revealed to not have any magnetic atom inside. These are discussed in more in Sec. ??.
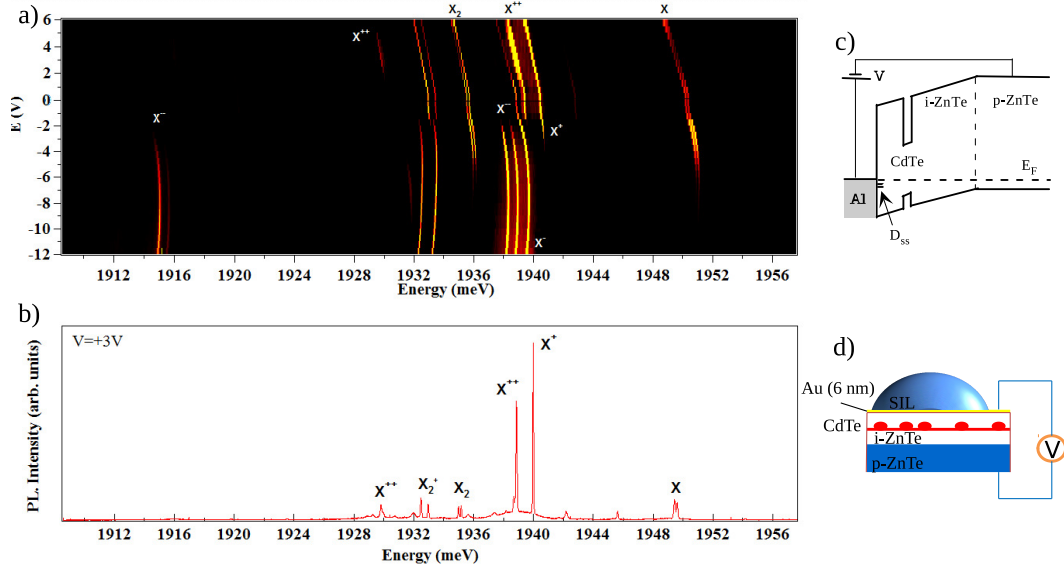
Figure I.6: (a) Evolution of the PL of a single dot under application of a bias voltage. (b) Spectra of the dot under application of a bias voltage V = +3 V. (c) Evolution of the energy structure of a CdTe dot and the i-ZnTe barrier under application of an electric field via the Schottky gate. (d) Schema of a charge control sample used for the μPL experiments.

I.3.2   Strain-free quantum dots

Strain-free quantum dots are formed by the thickness fluctuations of a CdTe quantum well in $Cd_xMg_{1-x}Te$ barriers. These fluctuations form steps localizing the carrier, acting as QDs. The higher the Cd concentration will be, the closer the lattice parameter will be, but it will also reduce the gap energy difference, reducing the confinement. The best strain to confinement ratio was found for CdTe QW in $Cd_{0.7}Mg_{0.3}Te$. The needed flux for this growth are shown in Tab. I.3.

Table I.3: Aimed flux for each cell during the growth of the strained samples.

Elements	Targeted BEP (Torr)
Cd	4.5×10^{-7}
Mg	1.6×10^{-8}
Te	5.26×10^{-7}

The strain-free sample were grown on an hybrid substrate. The substrate was made from a GaAs substrate, cleaned using H* plasma. We grew on it a CdTe

10

layer of about 3 μm, in order to recover the lattice parameter and not have defect close to the surface. With this thickness, the remaining strain in the layer should be of about 0.1% [9, 10]. A thin layer (about 7 nm) of ZnTe was grown between the GaAs and the CdTe in order to help the relaxation of strains [11]. The RHEED taken after the growth of the CdTe layer (Fig. I.7 (d)) shows sharp straight line, hinting at the recovery of a flat surface. A protective layer of amorphous Te was grown on the surface to keep it from being damaged outside the MBE chamber. It was removed at the beginning of the growth by evaporation.
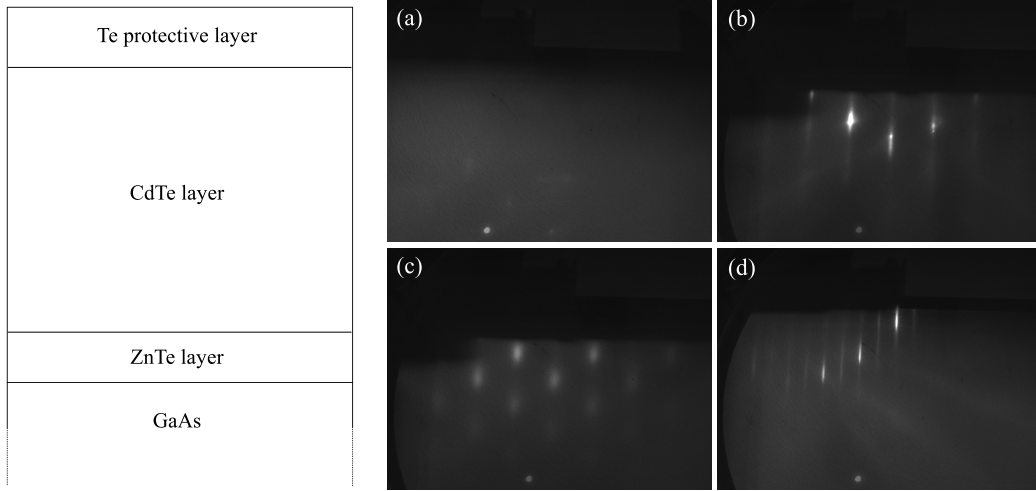

Figure I.7: Left: Layer structure of the hybrid substrate with its protective Te cap. Right: RHEED pattern taken at different key moment of the growth: (a) before H* cleaning of GaAs, (b) after H* cleaning of GaAs, (c) after the growth of the ZnTe layer, (d) after the growth of the CdTe layer.

We began to heat the substrate temperature to 300°C, in order to remove the protective amorphous Te layer. We waited a few second at this temperature to remove all the deposited Te, and then resumed the heating to go to 360°C. Starting at 320°C, we opened the Te cells in order to stabilize the surface. When the substrate temperature was stabilized at 360°C, we opened the Cd cells and grew a 2.35 μm layer of CdTe, in order to be as close as possible of a total lattice parameter recovery [9, 10].

We grew the first $Cd_{0.7}Mg_{0.3}Te$ barrier on this buffer layer. In order to be sure that there will be no relaxation in the quantum well, we choose to stick to the maximum cumulated thickness of the CdTe on a CdZnTe lattice, which has been shown to be lower than the one of CdTe on a CdMgTe lattice. This correspond to a maximum cumulated thickness of 130 nm [12]. We chose to grow 40 nm below the QW, and 90 nm above it, in order to have a thicker protective layer.

11

Once the 40 nm barrier layer was grown, we lowered the substrate temperature under Te flux. Growing the QW layer in a Te environment smooth the surface layer of the sample and help having a flat surface to grow the well. Once the substrate temperature reach respectively 295°C, we began the ALE of the QW. Two QW thickness was tested: either 4 ML or 2 ML. In both case, the growth was done growing CdTe layer as done for the strained sample, opening the Cr cell for 3 s for one cycle every two cycle. The whole recipe is described in Fig.I.8.
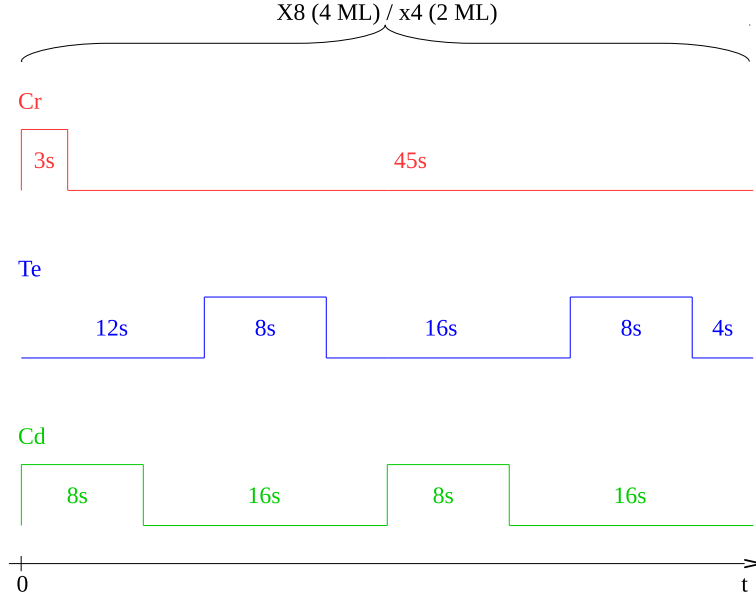

Figure I.8: Opening and closing cycles of each cell for the ALE of strain free (Cd,Cr)Te samples.

We then raised the substrate temperature up to 360°C, under a Te flux, in order to proceed to the growth of the upper barrier, acting also as a protective layer. The opening time was there calculated to grow 90 nm of $Cd_{0.7}Mg_{0.3}Te$.

Results

Four sample of strain-free dots doped with Cr were produced, listed in Tab. I.4.

The sample presented thin and intense peaks. It hints at a better confinement of the carriers in the QDs than what have been expected from dots formed by the thickness variation of a quantum well. This may be caused by higher steps than expected at the $CdTe/Cd_{0.7}Mg_{0.3}Te$ interface.

As discussed in Sec. **??**, the presence of a magnetic atom split the emission of

Table I.4: List of sample grown trying to incorporate Cr in SFD dots.

Sample	CdTe MLs	Cr aimed concentration (%)	Probability of Cr-doped QD
SFD4	4	0.35	None found
SFD5	2	0.15	None found
SFD6	2	0.54	None found
SFD7	2	0.35	None found
SFD8	2	0.75	None found

the exciton into several peaks, the number depending on the spin of the magnetic atom. However, such complex wasn't found in the strain-free samples. It may be caused by the the absence of static Jahn-Teller effect. In strain dots, this effect increase the probability of the Chromium to have a quantization axis the growth axis, z, making the splitting visible in our experimental setup. Without strain, the Jahn-Teller effect doesn't discriminate anymore between the three different axis, and thus the Chromium spin might have a quantization axis along the x or y. In this case, no splitting are visible for the quantum dot in our experimental setup, and the magnetic atom goes undetected.

In order to counter that, it was proposed to slightly strain the quantum well. This might be done by incorporating a low density of Zn in the $Cd_{0.7}Mg_{0.3}Te$ barrier. The strains created this way should be enough to increase the probability of quantization along the z axis, while staying negligible in regard of the Cr spin energy structure and dynamics. Such samples should be grown in the near future.

Conclusion

We saw in this chapter how we grew the samples that will be studied in the next chapters. We used the characterization of the samples done in Tsukuba to narrow on a Cr flux for the growth of Cr-doped QDs, and we decided to aim for a Cr estimated concentration in the sample of 0.17%. We then went to two other kind of sample: one allowing to apply an electric field on the dots, and on with strain free dots. The charge control sample growth was a partial success: we were able to apply an electric field on the sample, but no dot containing a single Cr was found. Strain-free dot presented promising fine peaks in their emission, but we were not able to find Cr in them either. More experiments will be done in order to successfully grow sample with the possibility of charge control, and strain-free dots.

In the next chapters, we will study with μ-PL dots found in the samples grown

in Grenoble (Chap. ??) and Tsukuba (Chap. ?? and ??).

Bibliography

[1] A. Cho and J. Arthur, "Molecular beam epitaxy", Progress in Solid State Chemistry **10**, 157–191 (1975).

[2] J. M. Hartmann, G. Feuillet, M. Charleux, and H. Mariette, "Atomic layer epitaxy of CdTe and MnTe", Journal of Applied Physics **79**, 3035–3041 (1996).

[3] J. Harris, B. A. Joyce, and P. Dobson, "Oscillations in the surface structure of Sn-doped GaAs during growth by MBE", Surface Science **103**, L90–L96 (1981).

[4] C. E. Wood, "RED intensity oscillations during MBE of GaAs", Surface Science **108**, L441–L443 (1981).

[5] R. D. Feldman, R. F. Austin, P. M. Bridenbaugh, A. M. Johnson, W. M. Simpson, B. A. Wilson, and C. E. Bonner, "Effects of Zn to Te ratio on the molecular-beam epitaxial growth of ZnTe on GaAs", Journal of Applied Physics **64**, 1191–1195 (1988).

[6] J. H. Chang, M. W. Cho, H. M. Wang, H. Wenisch, T. Hanada, T. Yao, K. Sato, and O. Oda, "Structural and optical properties of high-quality ZnTe homoepitaxial layers", Applied Physics Letters **77**, 1256–1258 (2000).

[7] F. Tinjod, B. Gilles, S. Moehl, K. Kheng, and H. Mariette, "II–VI quantum dot formation induced by surface energy change of a strained layer", Applied Physics Letters **82**, 4340–4342 (2003).

[8] P. Wojnar, C. Bougerol, E. Bellet-Amalric, L. Besombes, H. Mariette, and H. Boukari, "Towards vertical coupling of CdTe/ZnTe quantum dots formed by a high temperature tellurium induced process", Journal of Crystal Growth **335**, 28–30 (2011).

[9] K. Shigenaka, L. Sugiura, F. Nakata, and K. Hirahara, "Lattice relaxation in large mismatch systems of (111)CdTe/(100)GaAs and (133)CdTe/(211)GaAs layers", Journal of Crystal Growth **145**, 376–381 (1994).

[10] H. Tatsuoka, H. Kuwabara, Y. Nakanishi, and H. Fujiyasu, "Strain relaxation of CdTe(100) layers grown by hot-wall epitaxy on GaAs(100) substrates", Journal of Applied Physics **67**, 6860–6864 (1990).

[11] V. H. Etgens, M. Sauvage-Simkin, R. Pinchaux, J. Massies, N. Jedrecy, A. Waldhauer, S. Tatarenko, and P. H. Jouneau, "ZnTe/GaAs(001): growth mode and strain evolution during the early stages of molecular-beam-epitaxy heteroepitaxial growth", Phys. Rev. B **47**, 10607–10612 (1993).

[12] J. Cibert, R. André, C. Deshayes, G. Feuillet, P. Jouneau, L. S. Dang, R. Mallard, A. Nahmani, K. Saminadayar, and S. Tatarenko, "CdTe/ZnTe: critical thickness and coherent heterostructures", Superlattices and Microstructures **9**, 271–274 (1991).